Voltage stresses on PWM inverter fed induction motors : cable modeling and measurement

Roland Wetter, Basile Kawkabani, Jean-Jacques Simond

Institute of Energy Sciences, Swiss Federal Institute of Technology, Lausanne, Switzerland
EL-Ecublens, CH-1015 Lausanne, Switzerland phone: (+41) 21 693 2695, fax: (+41) 21 693 2050
e-mail: roland.wetter@epfl.ch

Abstract

The present paper deals with the determination of voltage stresses on PWM inverter fed induction motors by considering first the cable modeling and the measurement of different parameters. Then, based on this model, voltage stresses on the motor windings are determined precisely by an analytical approach, which takes into account the motor windings, and the filters. Different aspects related to such installations will be briefly described and discussed.

I. INTRODUCTION

An increasing part of low voltage standard induction motors operates with PWM voltage source inverters using IGBT transistors. This solution is applied to a wide range of power from 0.1 kW up to some MW. The supply of these induction motors by PWM inverters through cables leads to undesired overvoltages at the motor terminals. Considering classical transmission line analysis, and travelling-wave analysis with zero initial charges on cables, these transient overvoltages can reach usually twice the DC link voltage with a short rise time of about 200 ns. Nevertheless, depending on the cable parameters and on the length of the cable, these overvoltages may reach 3 or 4 p.u, and may lead to a failure of the insulation of the motor windings.

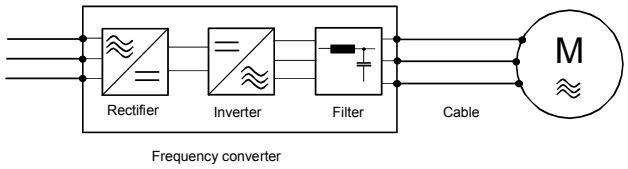

Figure 1. Studied system: (1) converter, (2) cable, (3) motor.

The prediction of the voltage stresses at the motor terminals depends on different installation parameters (Fig. 1), especially on those of the cable used for the connection between the inverter and the motor, as well as on the filter parameters at the output of the inverter. The cable manufacturer gives sometimes parameters for the cable such as inductances, capacitances and resistances. These
values are applicable close to the supplying network frequency (50/60 Hz). The determination of the high frequency properties of these cables becomes important in the case of variable speed drives with IGBT technology.

The parameters identification by finite element computations (FEM) has been performed on different cables. The results of this approach are compared with those given by measurements on the cables. The limits of numerical approaches will be discussed.

II. FEM APPROACH

Based on the detailed knowledge of the geometry and physical properties of phase conductors and of insulation materials, 2D FEM field calculations are performed, for symmetrical and unsymmetrical three-phase conductors. This approach has been applied on the cable shown in Fig.2.

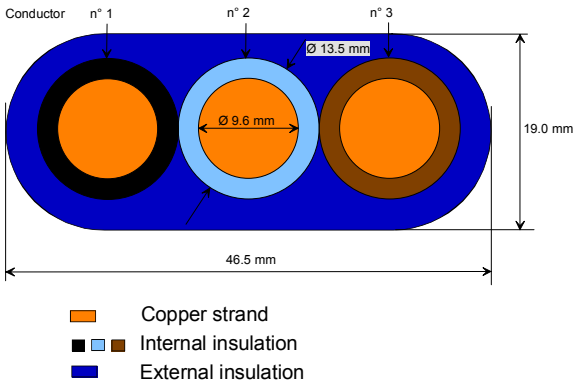

Figure 2. Cable n° 1. Pirelli SGFLT-0 3 x 50mm^2, 20.5 m

The determination of self and mutual inductances is obtained by using FEM computations in magnetostatics. The computations are based on the evaluation of the magnetic energy in a given volume surrounding the conductors.

The determination of capacitors between conductors is obtained from the electrical field strength. In this case, the electrostatic energy is considered. Except cables with armours connected to earth terminals, this approach is not able to evaluate precisely the capacitors between conductors and earth terminals. These ones depend strongly from the cable-laying and from the immediate surroundings of the cable (existence of conductive structures at other potentials).

The determination of the variation of the resistances and inductances as a function of the frequency is obtained by applying FEM computations in magnetodynamics. The skin effect obtained in this case will reduce the internal energy inside the conductors. For a single-core cable, the

skin effect may be calculated analytically by using the penetration depth.

On the other hand, for a multicore cable, if an alternating current is applied to a conductor, induced voltages and currents are obtained on the other conductors if there is a magnetic coupling between these conductors (fig. 3). The induced currents in the other conductors will generate losses and modify the penetration depth in these ones. Analytical approaches are not able to determine precisely this aspect.

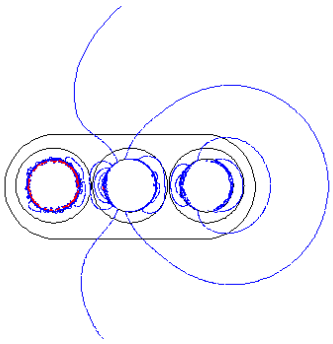

Figure 3. Distribution of the magnetic field when the lateral conductor situated on the left is supplied.

Like the electrostatic computations, the computations in magnetodynamics are not able to calculate the losses at high frequencies in conductive structures surrounding the cable if the position of these structures are not determined precisely (for example in the wire netting of a concrete flooring-tile or in the complex structures of a railway vehicle). Likewise, this approach may not determine dielectric losses.

III. HIGH FREQUENCY IMPEDANCE MEASUREMENTS

The best numerical model is only pertinent if it is confirmed by a set of measurements of various cases. Some parameters can be taken into account only with an experimental method. That's the case of traction drives which motors are generally supplied by three single-core cables situated in conductive longitudinal girders. In such cases, the best analytical approach is not able to determine precisely all the parameters.

The measurement of the cable parameters at high frequency is a challenge for the domain of high power electrical systems. The use of the low power measurement bridge is unsatisfying above about hundred kHz because the big disproportion of active losses in regard to the reactive values.

The proposed measurement method permits the determination of the parameters in the real operating modes of the cable. The three-phase equivalent circuit-diagram of a infinitesimal length of a three-phase cable (fig. 4) may be simplified. Indeed the switchings in the converters involve generally only two phases simultaneously. In most cases, the model may be reduced to the connection in series of two adjacent phases (fig. 5).

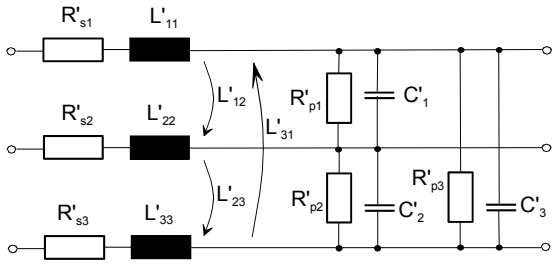

Figure 4. Equivalent circuit-diagram of an infinitesimal length dz of a three-phase cable.

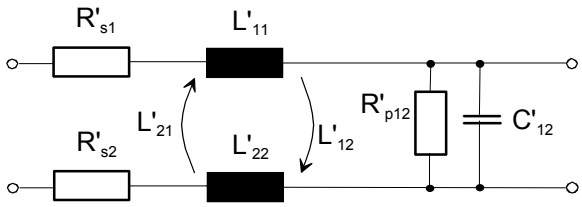

Figure 5. Simplified model.

The equivalent inductance of the circuit may be expressed by:

$$L'_{éq} = L'_{11} + L'_{22} - L'_{12} - L'_{21} \quad (1)$$

The equivalent circuit-diagram of a infinitesimal length is reduced to two impedances (fig. 6), given by:

$$\underline{Z}' = R'_{s1} + R'_{s2} + j\omega L'_{éq} \quad (2)$$

$$\underline{Y}' = \frac{1}{R'_{p12}} + j\omega C'_{12} \quad (3)$$

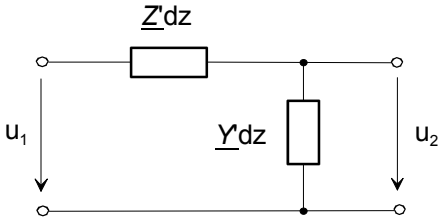

Figure 6. Equivalent circuit-diagram of an infinitesimal length *dz* of a cable.

The measurement method used is based on a wattmeter approach. For the measurement of the resistances and the inductances, two phases connected in series are supplied by a sinusoidal voltage with a variable frequency. In this case, the dielectric losses are negligible comparing to copper losses, and the reactive power due to the capacitors are negligible comparing to the one due to the inductances. The active and reactive power values permit to deduce the series resistances and inductances R'_{s1}, R'_{s2} et $L'_{éq}$.

This measurement principle is applied to the cable n° 1 (fig. 2). The measured resistance is larger than the one determined by FEM computations (fig. 7). This is due to the losses in the surroundings of the cable. Fig. 8 presents the value of the inductance.

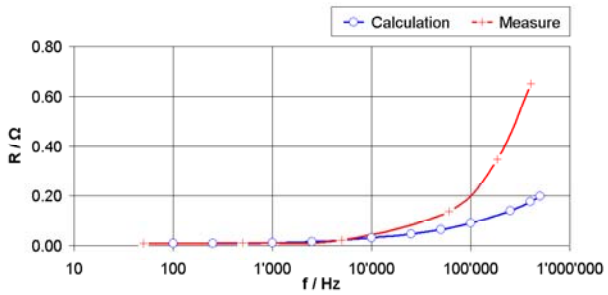

Figure 7. Comparison of calculated and measured values of Rs.

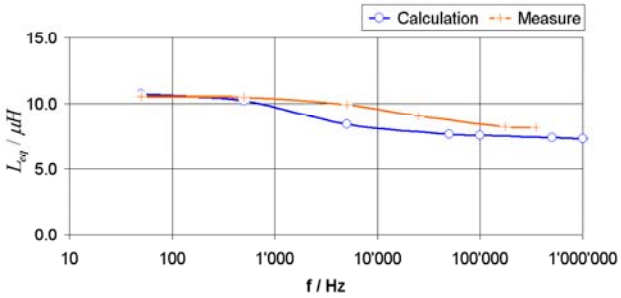

Figure 8. Comparison of calculated and measured values of L_{eq} (equivalent inductance of phases 1 et 2).

The value of the capacitor C'$_{12}$ is independent of the frequency. The measurement of this value at 50 or 60 Hz by the wattmeter approach mentioned above is precise enough. The measured value of the capacitor corresponds to an equivalent value of all the capacitors between two conductors as well as those between conductors and earth. (fig. 9).

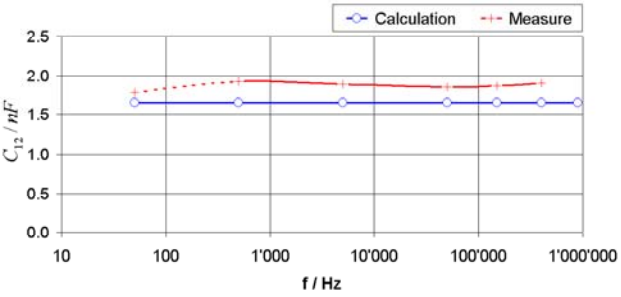

Figure 9. Comparison of calculated and measured values of C_{12}.

The difference between measurement and FEM computations is due to the fact that the measurement takes into account in addition to the capacitors between two conductors, those between the conductors and the earth. Depending on the surroundings of the cable, these capacitors vary passably, as well as the resonant frequency of the cable.

The dielectric losses are in most cases insignificant with regard to copper losses and skin effect. The dielectric losses measured by the wattmeter approach are precise enough for the modeling of the whole system, even if a relatively important error exists on the determination of these ones. The resistance measured is approximately equal to 1 GΩ for 1 m of cable.

IV. MODELING OF THE CABLE

The measured elements RLC are values corresponding to the elements of the equivalent circuit-diagram of an infinitesimal length dz, multiplied by the length of the cable. In order to determine the equivalent two-terminal-pair-network of the cable, it is necessary to convert the equivalent circuit-diagram of an infinitesimal length to an equivalent T or Pi model represented below (fig. 10).

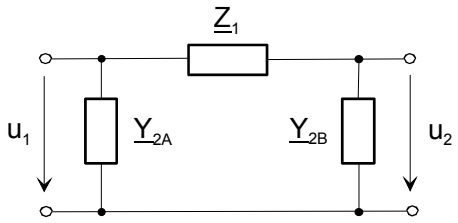

Figure 10. Equivalent two-terminal-pair-network of the cable.

The relations between the two above mentioned models are well known. For the Pi-model, one has:

$$\underline{Z}_1 = \underline{Z}_c \sinh(\underline{\gamma} \cdot d) \tag{4}$$

$$\underline{Y}_{2A} = \underline{Y}_{2B} = \frac{1}{\underline{Z}_c \coth(\underline{\gamma} \cdot d/2)} \tag{5}$$

with

d = length of the cable

$$\underline{Z}_c = \sqrt{\frac{\underline{Z}'}{\underline{Y}'}}$$

represents the characteristic impedance and

$$\underline{\gamma} = \sqrt{\underline{Z}' \cdot \underline{Y}'}$$

the propagation coefficient.
The values $\underline{Z}'$ et $\underline{Y}'$ are those defined in Fig 6.

It is interesting to note that in the equivalent circuit-diagram given in Fig. 10, the resistance of the admittance $\underline{Y}_2$ has no more direct link with the resistance of the dielectric losses R'_{p12}. It corresponds to an equivalent resistance depending at the same time of the series and parallel resistances. In the case of power cables, the influence of the series resistance is predominant. As an example, a series resistance for 1 m of cable is approximately equal to 0.1 Ω/m at high frequencies and the resistance in parallel 100 MΩ/m; these lead in the equivalent circuit with concentrated elements to a resistance in parallel which value is about 17.6 kΩ for a cable which length is equal to 16.6 m. This value remains practically unchanged if the resistance of the dielectric losses R'_{p12} varies ten times more or less. On the other hand, a variation of the resistances in series R'_{s1}, R'_{s2} produces a same variation on the resistance in parallel in the equivalent circuit-diagram of figure 10.

V. MODELING OF THE MOTOR

Given the high value of the inductance of the stator windings, the motor behaves as an antiresonant circuit for the high frequencies. Nevertheless, in spite of the high impedance represented by the motor at high frequencies, the input capacitor plays an important role as to the behavior of the system consecutive to a voltage jump. This input capacitor represents capacitors between phases as well as those between phases and earth. This equivalent capacitor decreases as function of the frequency and tends to an asymptotic value.

The measurement of the input capacitor is obtained also by a wattmeter method (fig. 11). The connection or not of the neutral doesn't influence the value of this capacitor. This fact confirms that only the capacitor value at the input of the motor has an influence on the overvoltage at high frequencies.

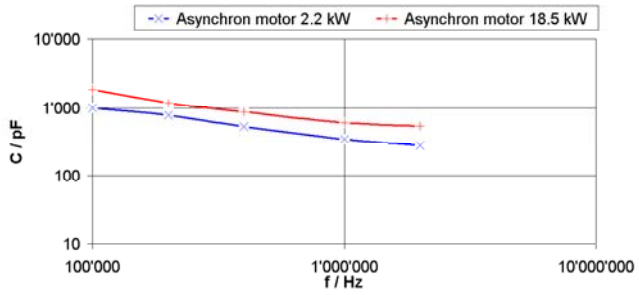

Figure 11. Measured input capacitor between two phases for two motors.

VI. MODELING OF THE WHOLE SYSTEM

In PWM inverter fed induction motors, there is generally a filter at least, at one of the ends of the cable. In order to keep the analysis method as simple as possible, the filters are reduced to equivalent two-terminal-pair-networks. So, they can be associated to the two-terminal-pair-networks of the cable and the motor.

The filters, cable and motor are represented each by a two-terminal-pair-network, defined by a matrix of impedance. The connection in cascade of different two-terminal-pair-networks leads to the determination of an equivalent one (fig. 12).

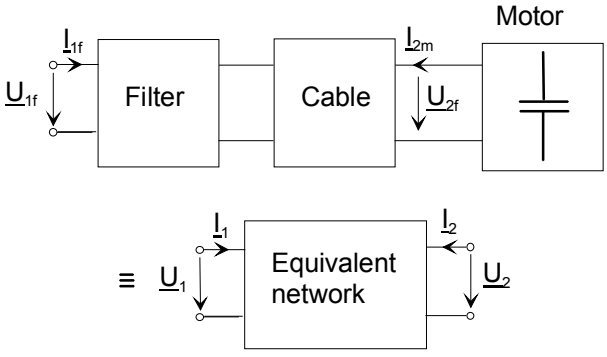

Figure 12. Modeling by using two-terminal-pair-networks.

The modeling of the filter, cable and motor is given by two-terminal-pair-networks as shown in fig. 13.

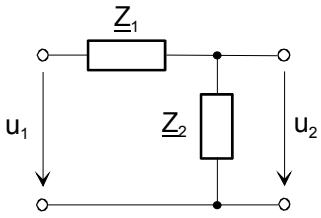

Figure 13. Elementary two-terminal-pair-network for filter, cable and motor.

For each two-terminal-pair-network, one has:

$$\begin{pmatrix} \underline{U}_1 \\ \underline{U}_2 \end{pmatrix} = \underline{M}_Z \begin{pmatrix} \underline{I}_1 \\ \underline{I}_2 \end{pmatrix} \tag{6}$$

with the matrix of impedance $\underline{M_Z}$ defined as follows:

$$\underline{M}_Z = \begin{pmatrix} \underline{Z}_1 + \underline{Z}_2 & \underline{Z}_2 \\ \underline{Z}_2 & \underline{Z}_2 \end{pmatrix} \tag{7}$$

In order to calculate the equivalent two-terminal-pair-network, it is necessary to use the matrix of chain $\underline{M_T}$. This one takes into account the voltages and currents at the ends of the two-terminal-pair-network:

$$\begin{pmatrix} \underline{U}_1 \\ \underline{I}_1 \end{pmatrix} = \underline{M}_T \begin{pmatrix} \underline{U}_2 \\ -\underline{I}_2 \end{pmatrix} \tag{8}$$

The matrix of chain is obtained from the transformation of the matrix of impedance. By considering the matrix of impedance in a generalized form:

$$\underline{M}_Z = \begin{pmatrix} \underline{Z}_{11} & \underline{Z}_{12} \\ \underline{Z}_{21} & \underline{Z}_{22} \end{pmatrix} \tag{9}$$

The matrix of chain becomes :

$$\underline{M}_T = \begin{pmatrix} \dfrac{\underline{Z}_{11}}{\underline{Z}_{21}} & \dfrac{\underline{Z}_{11}\cdot\underline{Z}_{22} - \underline{Z}_{12}\cdot\underline{Z}_{21}}{\underline{Z}_{21}} \\ \dfrac{1}{\underline{Z}_{21}} & \dfrac{\underline{Z}_{22}}{\underline{Z}_{21}} \end{pmatrix} = \begin{pmatrix} A & B \\ C & D \end{pmatrix} \tag{10}$$

The equivalent two-terminal-pair-network corresponding to the cascade of the filter, cable and motor is obtained by considering the product of the three respective matrices of chain:

$$\underline{M}_{T\,eq} = \underline{M}_{T\,filtre} \cdot \underline{M}_{T\,câble} \cdot \underline{M}_{T\,moteur} \tag{11}$$

The transfer function is then calculated directly from the matrix $\underline{M_{Teq}}$. Indeed, by considering the equations mentioned above, one has :

$$\underline{U}_1 = \underline{A} \cdot \underline{U}_2 - \underline{B} \cdot \underline{I}_2 \tag{12}$$

Now, the current I_2 is equal to zero at the high frequencies considered. Consequently, one obtains:

$$\frac{\underline{U}_2}{\underline{U}_1} = 1/\underline{A} \tag{13}$$

One can notice that many terms of the matrices are dependent on the frequency. The value of the series resistance must be known at least up to the resonant frequency of the system. In the case of lack of device which can measure this value of resistance at high frequencies, a satisfactory extrapolation model will be elaborated.

The resultant matrix of chain $\underline{M}_{T\,eq}$ is converted into a matrix of impedance and leads to an equivalent circuit-diagram similar to the one given in Fig 13. This circuit-diagram is strictly valid at the resonant frequency corresponding to the maximum of the transfer function. It can be used for the numerical simulation of the behavior of the system when a voltage jump is applied at the input of the system. The slope of the voltage jump corresponds to the one given by the converter. At the output of the equivalent two-terminal-pair-network, one obtains different stresses at the terminals of the motor: overvoltages, damping ratio, resonant frequency, and the gradient du/dt.

VII. CASES STUDIED

The parameters of a cable of traction with three single-core conductors (fig. 14) are measured, according to the method presented before, and for three cases:

a) conductors gathered together as a strand ;

b) conductors spaced in an overhead surrounding ;

c) conductors spaced and set on a reinforced concrete flooring-tile.

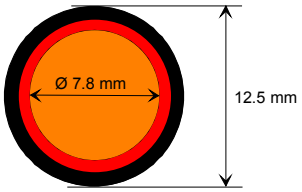

Figure 14. Traction cable Huber & Suhner RADOX 9 GKW-AX, 3.6 / 6 kV.

Considering the measured cable parameters, a simulation of the behavior of the system has been calculated when a voltage jump is applied at the input of the system, with the cable connected to the motors defined in fig. 11. These simulations have been performed by using MATLAB. A comparison between measurement and simulations is given in fig. 15 for different cases. For three cases, the motor is supplied with a frequency converter ABB ACS 300. For one case (fig. 15.b), the converter is the ABB ACS 550, which has a low voltage slope. Consequently, the overvoltage at the end of the cable is notably reduced.

For the case c), the measured value of the gradient du/dt is about twice the simulated one. A transient in the surroundings of the cable, corresponding to this particular frequency, may explain this difference. For the case d), the cable is exactly in the same situation, but the resonant frequency is lower and the discrepancy didn't occur again.

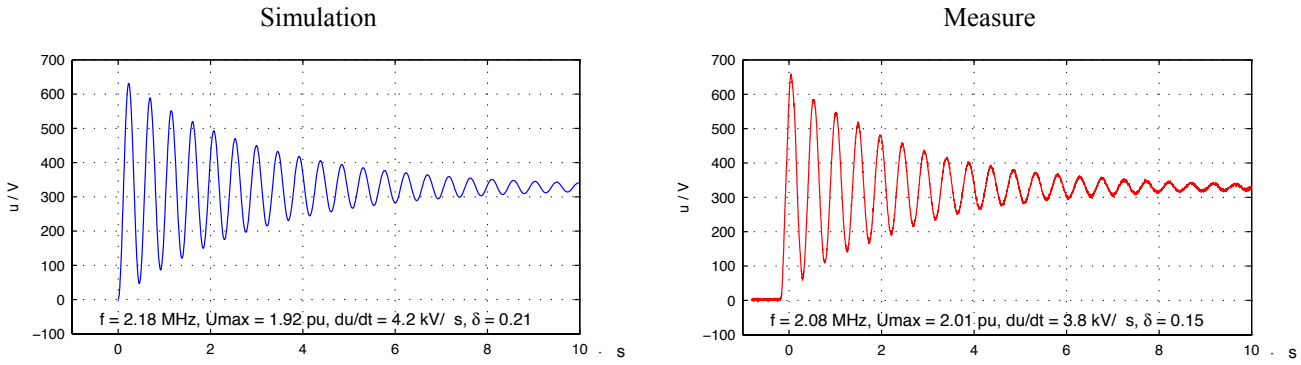

a) Conductors spaced in an overhead surrounding, ACS 300, motor 2.2 kW

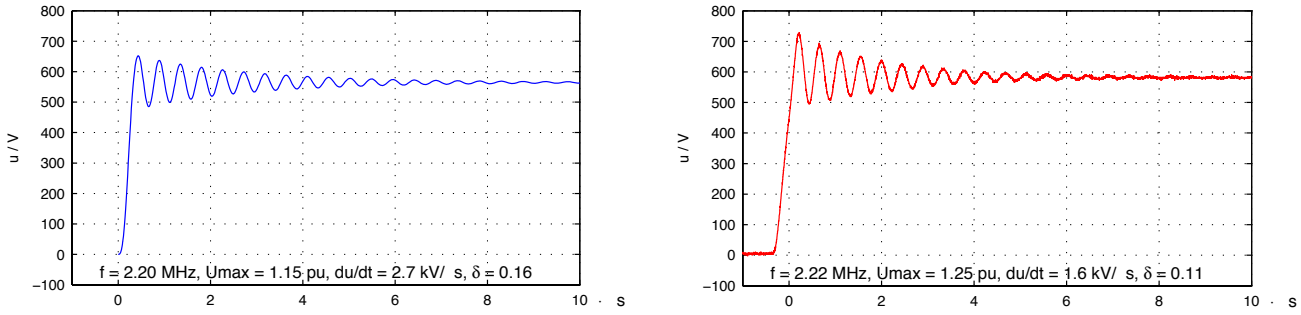

b) Conductors gathered together as a strand, on a reinforced concrete flooring-tile, ACS 550, motor 2.2 kW

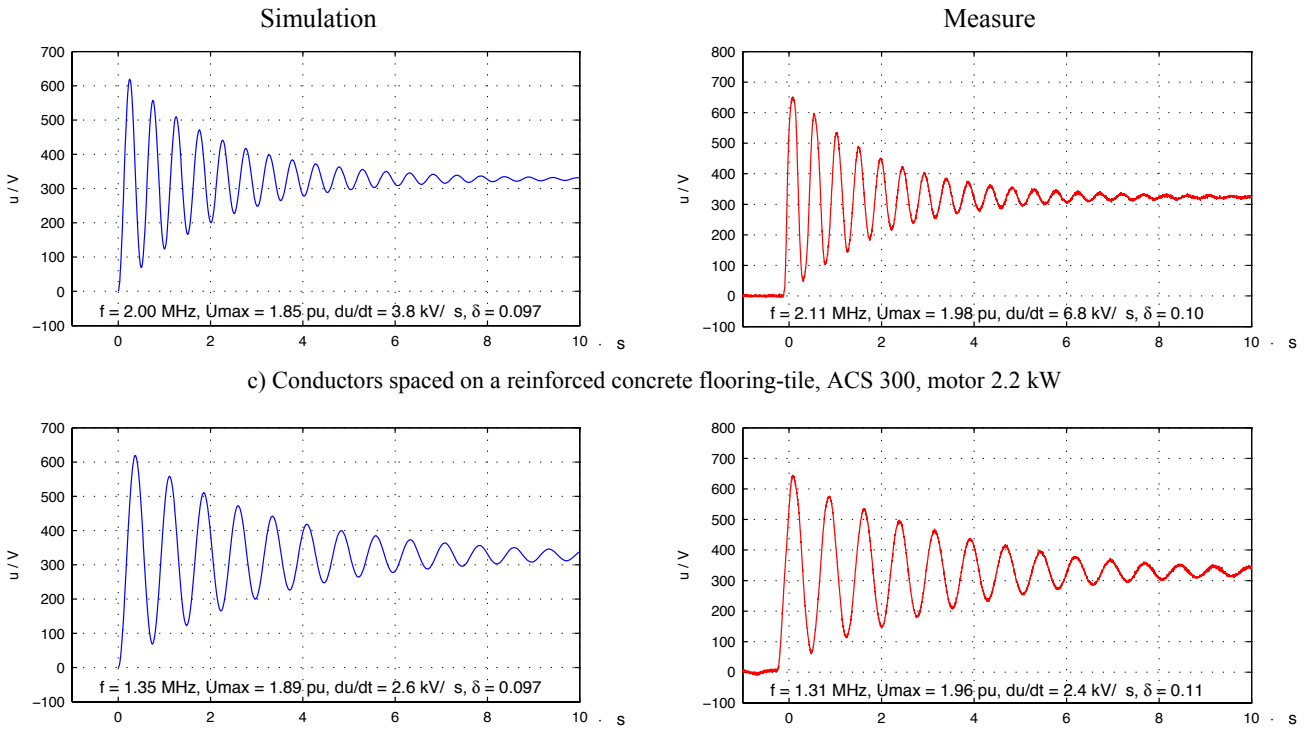

c) Conductors spaced on a reinforced concrete flooring-tile, ACS 300, motor 2.2 kW

d) Conductors spaced on a reinforced concrete flooring-tile, ACS 300, motor 18.5 kW

Figure 15. Measured and simulated voltage at the motor terminals, for a supply by converter.
The δ parameter is the voltage damping after 10 periods.

The comparison between measured and simulated results shows a good agreement. This confirms at the same time the modeling of the whole system, the validity of the measurement method and the theoretical comprehension of the phenomena observed in such installations.

The tools presented can be used without restriction for the determination of stresses on motors and cables, for the elaboration of filters, as well as for the analysis of lifetime.

Thanks to these tools, different observations partially known have been confirmed, especially:

- the slope of the voltage at the output of the converter modifies principally the amplitudes of the overvoltage. The overvoltage at the motor terminals decreases if the slope decreases too;

- the series resistance at high frequencies play a determinant role in the damping of the oscillation;

- the resonant frequency observed corresponds to the one of the whole system.

VIII. CONCLUSIONS

The present paper describes a global approach in order to avoid or minimize the risk of damage on PWM inverter fed induction motors in a planned installation. This approach consists on a precise determination of the cable parameters especially at high frequencies. The limits of an evaluation of the cable parameters by FEM computations have been specified if the structures surrounding the cable are not precisely defined. A measurement of the cable parameters in situ permits a precise determination of the cable parameters. The very good agreement of our simulations with the measured response confirms the validity of the elaborated tools.

These tools are able to determine precisely the stresses on the equipments of different drives with converters. In addition, they permit the elaboration of solutions in order to avoid unforeseeable damage on the equipments, due essentially to the fatigue and a premature decrease of lifetime.

IX. REFERENCES

[1] F. Gardiol, 'Electromagnétisme', *Traité d'électricité vol. III*, PPUR 1996, Lausanne, Switzerland.

[2] B. Kawkabani, J.-J. Simond, R. Wetter, 'Investigation of transient overvoltages of low induction motors due to IGBT-Inverter supply', *International Conference on Electrical Machines, (ICEM 2000),* vol. 2, pp. 1197-1200, August 2000, Espoo, Finland.

[3] J.-J. Simond, A. Sapin, B. Kawkabani, D. Schafer, M. Tu Xuan, B. Willy, 'Optimised design of variable speed drives based on numerical simulation', *EPE'97*, September 1997, Trondheim, Norway.